Journal of Materials Chemistry B

ROYAL SOCIETY OF CHEMISTRY

PAPER

View Article Online
View Journal | View Issue

Cite this: J. Mater. Chem. B, 2023, 11, 11300

Dual functional quaternary chitosans with thermoresponsive behavior: structure–activity relationships in antibacterial activity and biocompatibility†

Sedigheh Borandeh,‡ Isabella Laurén,‡ Arun Teotia, Jukka Niskanen and Jukka Seppälä *

Received 5th September 2023,
Accepted 7th November 2023

DOI: 10.1039/d3tb02066e

rsc.li/materials-b

Cationically modified chitosan derivatives exhibit a range of appealing characteristics, with a particular emphasis on their antimicrobial potential across a broad spectrum of biomedical applications. This study aimed to delve deeper into quaternary chitosan (QC) derivatives. Through the synthesis of both homogeneously and heterogeneously dual-quaternized chitosan (DQC), utilizing AETMAC ([2-(acryloyloxy)ethyl]-trimethylammonium chloride) and GTMAC (glycidyl trimethylammonium chloride), a permanent charge was established, spanning a wide pH range. We assessed structural differences, the type of quaternary functional group, molecular weight (M_w), and charge density. Intriguingly, an upper critical solution temperature (UCST) behavior was observed in AETMAC-functionalized QC. To our knowledge, it is a novel discovery in cationically functionalized chitosan. These materials demonstrated excellent antimicrobial efficacy against model test organisms *E. coli* and *P. syringae*. Furthermore, we detected concentration-dependent cytotoxicity in NIH-3T3 fibroblasts. Striking a balance between antimicrobial activity and cytotoxicity becomes a crucial factor in application feasibility. AETMAC-functionalized chitosan emerges as the top performer in terms of overall antibacterial effectiveness, possibly owing to factors like molecular weight, charge characteristics, and variations in the quaternary linker. Quaternary chitosan derivatives, with their excellent antibacterial attributes, hold significant promise as antibacterial or sanitizing agents, as well as across a broad spectrum of biomedical and environmental contexts.

1. Introduction

Chitosan finds wide use in medicine and biomedical applications due to its distinct properties. This polysaccharide and its derivatives offer numerous advantages, including high availability, low toxicity, cationic charge, and biocompatibility.[1] The ionic charge from *N*-acetylglucosamine and glucosamine contributes to its antimicrobial and coagulation/flocculation properties.[2] However, the practical applications of chitosan are limited by its pH-dependent water solubility, poor mechanical strength, and acid resistance. These constraints can be addressed by introducing specific functional groups to achieve desired chemical and physical properties. The incorporation of cationically charged moieties significantly enhances water solubility and antimicrobial/flocculation properties, thereby improving its antimicrobial effectiveness.[3,4]

Quaternary ammonium compounds are well-known for their antimicrobial properties due to their cationic charge.[5] By replacing chitosan's amino terminals with quaternary ammonium functional groups, a permanent cationic charge is introduced, improving water solubility across a broad pH range and enhancing antimicrobial properties.[6,7] Various methods have been developed over time to quaternize chitosan, each with advantages and disadvantages influencing the resulting properties. Common approaches include using methyl iodide to prepare *N*,*N*,*N*-trimethyl chitosan (TMC), or with glycidyl trimethyl ammonium chloride (GTMAC) or 3-chloro-2-hydroxy-propyl trimethyl ammonium chloride (CHPTMAC) to form *N*-[(2-hydroxy-3-trimethyl ammonium)propyl] chitosan (HTCC).[8,9] However, TMC requires strong alkaline conditions and methyl iodide is highly toxic. Formaldehyde and sodium borohydride used in TMC formation are also toxic.[10,11]

Polymer Technology, School of Chemical Engineering, Aalto University, Kemistintie 1, 02150 Espoo, Finland. E-mail: jukka.seppala@aalto.fi

† Electronic supplementary information (ESI) available: Reaction schemes of quaternized chitosan (Scheme S1); FTIR spectra (Fig. S1); ^{1}H NMR spectra (Fig. S2); ^{13}C NMR spectra (S3); plotted GPC data of the molecular weight (Fig. S3); TGA thermogram curves and X-ray diffraction patterns (Fig. S5); UCST behavior (Fig. S6); antimicrobial analysis (Fig. S7); cytotoxicity analysis (Fig. S8); quantitative live/dead analysis (Table S1). See DOI: https://doi.org/10.1039/d3tb02066e

‡ S. B. and I. L. contributed equally to this work.

The complexity of synthesis, expensive reagents, harsh conditions, and concerns about toxicity and biocompatibility hinder practical applications in biomedicine. Previously, chitosan was quaternized with [2-(acryloyloxy)ethyl]-trimethylammonium chloride (AETMAC) in an aqueous environment.[12] Unlike previous methods, AETMAC has minimal reported toxicity and no major hazard classifications; it is not widely used in chitosan-based biomedical applications. Hassan (2018) describes the preparation of chitosan films grafted with AETMAC to improve antibacterial properties, although only in a single-quaternized manner and without any structure–property correlations.[13] Aza-Michael reactions of chitosan, on which AETMAC-functionalized chitosan is based, are described in other reports.[14,15]

In this study, we quaternized chitosan with AETMAC in O- and N,O-positions, yielding single- and homogenously double-quaternized chitosan (SQC and DQC). Additionally, heterogeneously DQC was achieved using both AETMAC and GTMAC. This synthesis route and the antiviral efficacy of the resulting quaternary compounds were explored in our previous study.[16] The primary aim of this work was to improve the quaternization efficiency and study antibacterial activity, biocompatibility, and structure–property relationships. This work demonstrated the superiority of the AETMAC approach over GTMAC in physical properties, solubility, and the property-antibacterial activity relationship against *P. syringae* and *E. coli*. The impact of functional group type, position, and degree of quaternization on chitosan's structure and properties were evaluated. Furthermore, the cytotoxicity of AETMAC derivatives on NIH-3T3 mouse fibroblast cells was assessed, although cytotoxicity is of greater relevance in other implementations, *e.g.* in pharmaceutical and medical applications. These compounds, when used as surface coatings, unlike conventional surface disinfectants, can offer enduring protection against microbes due to their inherent antimicrobial activity and lower toxicity. Such derivatives are well-suited for applications like surface disinfectants or antimicrobial agents in biomedicine.

2. Experimental

2.1. Materials

Chitosan (CAS no. 9012-76-4; degree of deacetylation DDA ≥ 75%; purity: 99%) was purchased from TCI (Japan) and used without further purification. GTMAC, AETMAC, dimethyl sulfoxide-d_6 (DMSO), deuterium oxide (D_2O), ammonium persulfate (APS), and 2-propanol were purchased from Sigma Aldrich (USA). Acetic acid (99–100%), acetone, and methanol were supplied by VWR Chemicals (USA). Sodium hydroxide (NaOH), benzaldehyde (C_7H_6O), and sodium hydrogen carbonate ($NaHCO_3$) were obtained from Merck (Germany). Chloroacetic acid (99+%) was supplied by Acros Organics (USA). Hydrochloric acid 4 M (HCl) was purchased from Fluka Analytical (Switzerland). *Escherichia coli-C* (Cat. no. 124400) was purchased from Carolina Biological (USA), and *Pseudomonas syringae* (Cat. no. 21482) was purchased from DSMZ-German Collection of Microorganisms and Cell Cultures (Germany). Luria-Bertini broth was purchased from Condalab (Spain). Dulbecco's Modified Eagle Medium (DMEM) (cat no. D6429), penicillin (10 000 U mL^{-1})–streptomycin (10 mg mL^{-1}) solution, trypsin-ethylenediaminetetraacetic acid (TE) (1×), phosphate-buffered saline (PBS), fluorescein diacetate (FDA), propidium iodide (PI), and 3-(4,5-dimethylthiazol-2-yl)-2,5-diphenyltetrazolium Bromide (MTT) were purchased from Sigma-Aldrich (USA).

2.2. Quaternization of chitosan

2.2.1. Synthesis of Schiff base chitosan. To successfully synthesize QC in both the O-position (SQC) and in the N,O-position (DQC), the amine group of pure chitosan was protected using benzaldehyde, resulting in Schiff base chitosan (*N*-benzylidene-chitosan). The preparation of Schiff base chitosan followed the methods described by Fu *et al.* (2011),[17] using a ratio of 1.0 g (6.2 mmol) of chitosan and 6.6 g (67.8 mmol) of benzaldehyde. The successful synthesis of Schiff base chitosan was confirmed using FT-IR, where the characteristic peak of the C=N band appeared at 1640 cm^{-1} (Fig. S1 and Scheme S1, ESI†).

2.2.2. Synthesis of single and double quaternized chitosan with AETMAC (SQC- and DQC-AETMAC). Chitosan was quaternized through the graft polymerization of AETMAC onto the chitosan backbones, as described in our previous study.[16] To ensure quaternization in the O-position, Schiff base chitosan served as the starting material. Schiff base chitosan (1.0 g, 4.0 mmol) was dissolved in 2% acetic acid in D_2O (100 mL) at 80 °C. APS (1.0 g, 4.4 mmol, as redox initiator) and AETMAC (2.0 mL, 11.7 mmol) were gradually added to the solution and stirred for 3 h at 80 °C under a nitrogen (N_2) atmosphere. After cooling to room temperature, the product was neutralized with NaOH and precipitated with acetone. To remove unreacted AETMAC monomers and poly-AETMAC by-products, the product was washed with methanol and freeze-dried for 24 h. After quaternization in the O-position, the protected amine was deprotected by suspending the compound in a 0.1 M solution of HCl in ethanol overnight. The product was neutralized with NaOH and freeze-dried, resulting in SQC-AETMAC. To successfully quaternize the SQC-AETMAC in the N-position and generate DQC-AETMAC, the polymerization process was repeated using SQC-AETMAC (1.0 g, 3.2 mmol) as starting material (Scheme 1 and Scheme S1, ESI†).

2.2.3. Synthesis of single and double quaternized chitosan with GTMAC (SQC- and DQC-GTMAC). Chitosan quaternized with GTMAC was synthesized as previously described by Spinelli *et al.*,[18] with modifications. As mentioned earlier, Schiff base chitosan was used as the starting material to prevent the functionalization of the amine. Here, Schiff base chitosan (1.0 g, 4.0 mmol) and GTMAC (3.8 g, 25.1 mmol) were distracted in isopropanol (50 mL) and allowed to react for 30 h at 70 °C. The resulting product was precipitated and subsequently washed several times in an acetone–ethanol solution (1 : 1) and then freeze-dried (Scheme 1 and Scheme S1, ESI†). The protection of the amine was removed as described earlier, but a

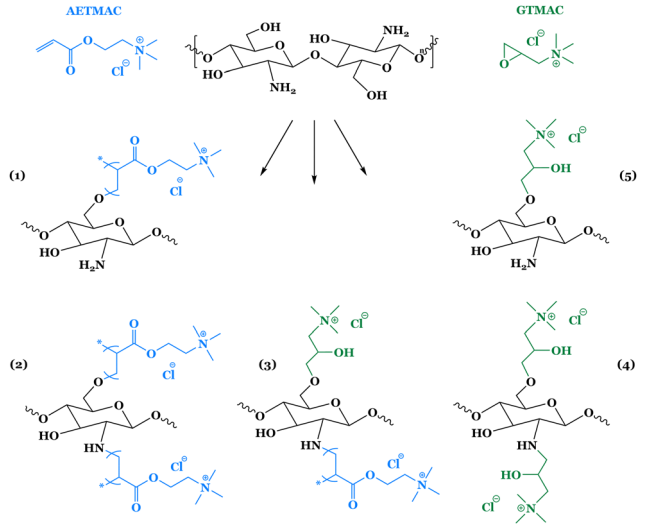

Scheme 1 Schematic representation of quaternized chitosan, where 1–5 is SQC-AETMAC, DQC-AETMAC, DQC-GT/AET, DQC-GTMAC, and SQC-GTMAC. Full reaction schemes are provided in ESI.†

0.25 M solution instead of 0.1 M HCl in ethanol. The GTMAC synthesis step was repeated to generate DQC-GTMAC with quaternary groups in both O- and N-positions (Scheme 1 and Scheme S1, ESI†).

2.2.4. Synthesis of heterogeneously double quaternized chitosan with AETMAC and GTMAC (DQC-GT/AET). To generate heterogeneously double-quaternized chitosan, chitosan was quaternized with GTMAC in the O-position and AETMAC in the N-position. The synthesis steps were similar to previous descriptions of GTMAC and AETMAC reactions (Scheme 1 and Scheme S1, ESI†).

2.3. Characterization

^{1}H and ^{13}C NMR spectroscopy. ^{1}H NMR analyses were performed with a Bruker Avance III 400 spectrometer and ^{13}C NMR was determined with Bruker Avance NEO 600 (Bruker, USA). Chitosan was dissolved in 2 wt% DCl/D_2O, whereas QCs were dissolved in D_2O.

FT-IR spectroscopy. Fourier transform infrared spectra (FT-IR) were determined with a Spectrum Two FT-IR Spectrometer (PerkinElmer, UK), using an attenuated total internal reflection (ATR) equipped with a diamond window. The samples were fully ground and scanned in the range of 4000–400 cm^{-1}, at a resolution of 4 cm^{-1} and 32 accumulations.

Zeta potential and particle size measurement. The zeta potential was analyzed with Zeta sizer Nano ZS 90 (Malvern Panalytical, UK). The potential was measured over a pH range of 3.0–8.5, and the samples were dissolved in distilled water. The influence of temperature on the solution's particle size was analyzed using backscattering with a Zeta sizer Nano ZS (Malvern Panalytical, UK) at an angle of 173°. The solution was heated/cooled at a rate of 1 °C min^{-1} from 10–70 °C and equilibrated for 2 min before measurement at 5 °C intervals.

Thermogravimetric analysis (TGA). The thermogravimetric analysis was conducted on a TGA Q500 thermogravimetric analyzer (TA Instruments, USA). The heating rate was 10 °C min^{-1} from 30–800 °C under N_2.

X-ray diffraction (XRD). The X-ray diffraction was carried out on an X'PERT PRO MPD Alpha 1 (Malvern Panalytical, UK) with Cu Kα radiation at 40 mA and 45 kV at 25 °C. The scanning rate was 4 °C min^{-1} and the scope was from 5 to 100° (2θ).

Rheological analysis. The viscosity was measured using a Physica MCR 301 rheometer (Anton Paar, Austria), using a 50 mm diameter parallel plate geometry at 25 °C. The working concentration was 50 mg mL^{-1}. Chitosan was dissolved in acetic acid (1% w/v), whereas the other materials were dissolved in deionized water for 12 hours before analysis.

Transmittance measurements. The cloud points (T_{cp}) were determined by measuring the transmittance of the solutions as a function of temperature using a J-1500-150ST CD-spectrometer equipped with a temperature-controlled cell along and a magnetic stirrer (JASCO, Japan). A cooling/heating rate of 1 °C min^{-1} was applied with a 30 second equilibration at each temperature interval before triplicate transmittance measurements at 660 nm. The cloud points were determined at 50% transmittance. The solutions of SQC-AETMAC (1.25, 2.5, 5, and 10% (w/v)) in Milli-Q water and 10% with 0.5 or 1.0 M NaCl were prepared and equilibrated at 80 °C for 10 minutes before measurements. The pH of the solutions was not adjusted and was measured between pH 1.2–2.0.

Antimicrobial activity analysis. The antimicrobial activity of QCs was assessed at different concentrations using *P. syringae* and *E. coli*-C as model organisms. These organisms were chosen due to laboratory safety considerations (biosafety level-1). The antimicrobial activity against *P. syringae* and *E. coli* was evaluated through both zones of inhibition and microdilution assays to determine the minimum inhibitory concentration (MIC) and the minimum bactericidal concentration (MBC) of the compounds. The antimicrobial activity remained well below the T_{cp} for the materials.

For the microdilution assay, *E. coli* and *P. syringae* were cultured in Luria-Bertani (LB) broth until reaching an OD_{600} of 0.1 ($\sim 1 \times 10^8$ CFU mL^{-1}, colony forming units). The materials were dissolved in 1× phosphate-buffered saline (PBS, pH 7.4) and titrated to assess their antimicrobial activity. Wells containing 100 μL of the test compound at concentrations ranging from 0.5 to 20% (w/v) in LB were inoculated with 1×10^6 CFU mL^{-1} of microbial cells and incubated for 10 minutes (contact time), or for 12 hours to estimate MIC and MBC values. After the required incubation time, 900 μL of a neutralizing solution (containing peptone (1 g L^{-1}), lecithin (0.7 g L^{-1}), Tween-80 (5.0 g L^{-1}), and sodium thiosulphate (1 g L^{-1})) was added and mixed. The mixture was then added to 3 mL of LB-agar maintained at 50 °C, mixed thoroughly, and pour-plated on LB-agar plates using a dual agar overlay method, or 100 μL of the culture medium was spread-plated on the LB plates, either directly or after appropriate dilutions to estimate viable CFUs. *E. coli* was incubated at 37 °C and *P. syringae* at 30 °C. The samples were observed for colony formation after 24, 48, and 72 h of incubation. The number of bacterial colonies observed

was used to calculate the percentage of inhibition (removal) using eqn (1).

$$\text{Removal}\,(\%) = \left[\frac{\text{Initial CFUs} - \text{Final CFUs}}{\text{Initial CFUs}}\right] \times 100. \quad (1)$$

For the streak plate assay, the required amount (5 and 10% (w/v)) of the active compound was dissolved in sterile distilled water and used for the activity assay. *E. coli* was cultured on LB agar and inoculated either by streaking or spreading. A 10 μL solution of QC was spotted on the *E. coli*-seeded LB plates and incubated overnight at 37 °C. The plates were observed for inhibition of microbial growth (zone of inhibition) the following day.

***In vitro* cytotoxicity/cell viability evaluation.** The cytotoxicity of the pure QCs was estimated through three distinct methods. Initially, fibroblast cells were exposed to various QC concentrations, and their response was observed directly under a microscope. Subsequently, the cell viability and metabolic activity were assessed using an MTT assay. Finally, live–dead staining of cells exposed to QCs at different concentrations and durations was performed to evaluate cytotoxicity.

For morphological analysis, NIH-3T3 fibroblasts were cultured in a flat-bottom 96-well cell-culture treated plate. Each well contained 100 μl DMEM complete medium (FBS 10% v/v, penicillin, and streptomycin) and was seeded with approximately 1×10^4 actively growing fibroblasts. The cells adhered and proliferated for 48 h in a humidified CO_2 (5%) environment at 37 °C before conducting the tests. QCs were dissolved in PBS (1×) at a concentration of 20 mg mL^{-1} (stock solution) and were used immediately after dissolution. The spent medium in the wells was replaced with 100 μl of fresh DMEM complete medium, and 100 μl of the stock solution was added, mixed thoroughly, and added to three different wells (triplicate sample preparation), resulting in an effective concentration of 10 mg mL^{-1}. From these wells, further serial dilution was carried out in subsequent wells, creating a concentration gradient (10, 5, 2.5, 1.25, 0.65, 0.31, and 0.15 mg mL^{-1}) of the compound in the wells. The cells were visualized using an inverted microscope (Leica, Germany) after 24 and 48 h of exposure, observing changes in cell morphology as a result of the compound concentration and exposure time. All the tests were carried out in triplicate and repeated at least once (n = 6).

Cytotoxicity of the QCs was further assessed by performing live–dead staining (FDA/PI) of the NIH-3T3 fibroblasts exposed to different QC concentrations for 48 h. The cells were cultured in an 8-well chamber slide (cat no. 155409, Nunc, USA). NIH-3T3 cells were seeded at a density of $\sim 1 \times 10^4$ cells per well, containing 200 μl of DMEM complete medium. The cells adhered and proliferated for 48 h in a humidified CO_2 (5%) environment at 37 °C. Appropriate volumes of the stock solution of DQC were added to the first well of the chamber slide and mixed gently, achieving a working concentration of 2.0 mg mL^{-1}. Serial dilutions were performed in subsequent wells, generating a concentration gradient of 2.0, 1.0, 0.5, and 0.25 mg mL^{-1} per well. A 48 hours exposure was considered as the endpoint for the test based on results obtained from a direct visualization experiment. After 48 h, the cells were gently washed with PBS (1×), and live–dead staining was performed using FDA and PI stains diluted in DMEM medium, following the manufacturer's instructions. The tests were conducted in duplicate. Imaging was carried out with a fluorescent microscope equipped with green and red filter channels (Leica, Germany). Image segmentation and quantification were performed using Fiji software.[19]

The cytotoxicity of different QCs was further evaluated by conducting an MTT-based viability assay on the cells exposed to different QC concentrations for 24 and 48 h. The cells were cultured in cell-culture treated 96 well flat-bottom plates in 100 μL of DMEM medium, as mentioned above, and exposed to various QC concentrations (5.0, 2.5, 1.25. 0.62, 0.31, and 0.15 mg mL^{-1}) generated by serial dilution. After the designated contact time (24 or 48 h), the medium was removed, and 50 μL of MTT reagent (1.0 mg mL^{-1}, medium) was added to each well and incubated for 4 h. The reagent was then removed, and the formazan product was dissolved in DMSO (200 μL $well^{-1}$). The metabolic activity of the cells (viability) was evaluated by measuring OD_{570} using a multi-well plate reader (Eon, BioTek Instruments, USA), after a 1 : 1 dilution in fresh DMSO in a new 96-well plate. Cells cultured in only DMEM complete medium served as a positive control, and DMSO served as a blank control.

3. Results and discussion

3.1. Structural characterization

3.1.1. FT-IR spectra. FT-IR analysis was used to confirm the introduction of quaternary compounds into chitosan (Fig. 1(A) and Fig. S1, ESI†). Following quaternization, the NH_2 band at 1598 cm^{-1} disappeared, which can be ascribed to the deformation of the primary amine vibration (N–H) in the amide II band, indicating the reaction of NH_2 in chitosan with the quaternary compound. The band around 1645 cm^{-1} confirms the presence of residual *N*-acetyl groups on the CS structure, considering the manufacturer's reported value of a DDA ≥ 75%. For the QCs, a new peak emerged at 1479 cm^{-1}, likely attributed to the methyl

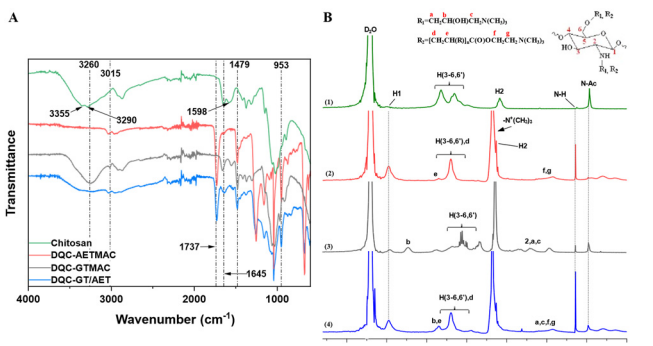

Fig. 1 (A) FT-IR spectra, and (B) ^{1}H NMR spectra of chitosan and its double quaternized derivatives, where 1–4 are chitosan, DQC-AETMAC, DQC-GTMAC, and DQC-GT/AET.

group of the introduced quaternary ammonium. Additionally, the vibrations ascribed to the primary amine at approximately 3355 and 3290 cm^{-1} disappeared after modification, and two new bands appeared at 3260 and 3015 cm^{-1}, presumably attributed to the secondary amine. The characteristic band of the two hydroxyl groups between 1152 and 1030 cm^{-1} remained unchanged, suggesting the substitution occurred at the amino group rather than the hydroxyl groups. These results are consistent with previous reports and confirm the successful quaternization of chitosan.[20,21] Chitosan quaternized with AETMAC showed two bands likely ascribed to the C=O vibration of the ester group and a C–N vibration of the quaternary ammonium group at 1737 and 953 cm^{-1}, respectively. This further confirms the successful introduction of AETMAC to the chitosan structure.[22]

3.1.2. ^{1}H and ^{13}C NMR. ^{1}H-NMR was used for structural characterization and to estimate the degree of quaternization of the modified chitosan (Fig. 1(B) and Fig. S2, ESI†). The signals at 4.50 ppm (H1); 3.40–4.00 ppm (H3–6); 3.15 ppm (H2); 2.10 ppm (N–H) and 1.91 ppm (*N*-acetyl) are assigned to the chitosan skeleton.[13] The degree of deacetylation (DDA) was determined using eqn (2), where $[CH_3]$ and [H2, H3–H6, H6′] are the integrals corresponding to the acetyl peak of the GlcNAc unit and the pyranose protons (Fig. S2, ESI†).[16,23] The calculated average DDA of chitosan was ≈74.3%, which is in close agreement with the manufacturer's reported value of ≥75%.

$$\mathrm{DDA} = \left[1 - \frac{[CH_3]/3}{[\mathrm{H2, H3-H6, H6'}]/6}\right] \times 100\% \qquad (2)$$

For the quaternized derivatives, the signals found at approximately 4.50 ppm (H1); 3.60–3.80 (H3-6 for GTMAC-QCs); 3.65 (H5 and N^+–CH_2–CH_2–O– stretch from AETMAC-QCs); 3.15 ($N^+(CH_3)_3$); 3.00 (H8); and 2.00 (*N*-acetyl), confirm the introduction of both AETMAC and GTMAC to chitosan.[13,20,22] The signal found at 4.65 ppm is attributed to the solvent (D_2O). The degree of quaternization (dQ) can be altered to achieve specific properties. The dQ, as well as the subsequent charge density, can affect the solubility, viscosity, and antimicrobial properties of chitosan. Here, the dQ was determined from the ^{1}H-NMR integrals (Fig. S2, ESI†) using eqn (3):

$$\mathrm{dQ} = \left[\frac{-N^+(CH_3)_3 \times 6}{[\mathrm{H2, H3-H6, H6'}] \times 9}\right] \qquad (3)$$

where $-N^+(CH_3)_3$ is the integral attributed to the quaternary ammonium group, at approximately 3.15 ppm, and [H2, H3–H6, H6′] is the integral area of the signal attributed to the pyranose protons found approximately between 3.3–4.0 ppm.[24,25] The calculated dQ values for all QCs are presented in Table 1. DQC derivatives showed higher dQ values compared to SQCs, indicating successful double quaternization of chitosan. Notably, AETMAC-functionalization yielded a higher dQ than the GTMAC derivatives. GTMAC was grafted onto the chitosan structure as direct functional modification, whereas AETMAC was introduced through a radical polymerization reaction in which vinyl groups created new chain branches from the parent glucosamine unit (Scheme 1).

Table 1 The degree of quaternization (dQ), weight averaged molecular weight (M_w), and dispersity ($Đ$) of chitosan and its derivatives

Samples	dQ	M_w (kDa)	$Đ$
Chitosan	—	59.3	2.4
SQC-GTMAC	0.5	34.7	2.2
DQC-GTMAC	1.1	25.0	2.7
SQC-AETMAC	0.9	5.1	1.4
DQC-AETMAC	1.7	7.3	1.4
DQC-GT/AET	1.1	12.9	1.4

Functionalization of the amine (C-2) and the –OH (C-6) is favored due to lower steric hindrance, compared to the –OH group at C-3. This was also confirmed by ^{13}C NMR analysis (Fig. S3, ESI†), where the intensity of the C-6 signal (at approximately δ = 62 ppm) was significantly higher than that of C-3 ($\delta \approx 73$ ppm). This was consistent with previous determinations.[16,26] Additionally, the change in the downfield shift of the C-6 position from $\delta \approx 58$ ppm in chitosan to $\delta \approx 62$ ppm in QC confirms quaternization.

3.1.3. Molecular weight. The molecular weight (M_w) significantly affects the antimicrobial activity and flocculation properties of chitosan. The M_w of the prepared QCs was determined using GPC (gel permeation chromatography),[16] and is presented in Table 1 and Fig. S4 (ESI†). DQC-GTMAC has a lower M_w compared to SQC-GTMAC, possibly due to longer reaction times and therefore harsher conditions causing fragmentation of the parent chitosan chain. In contrast, DQC-AETMAC exhibited a higher M_w than SQC-AETMAC due to the formation of poly-AETMAC branches during polymerization. For antimicrobial properties, a low M_w is preferable. Previous reports suggest that chitosan's antimicrobial properties increase as the M_w decreases.[27–29] Low M_w chitosan, ideally below 5 kDa, can penetrate the microbial cell walls, disrupting intracellular activity and affecting RNA, protein synthesis, and mitochondrial functions.[30]

3.1.4. Zeta potential. The cationic charge of chitosan is a factor influencing its antimicrobial and flocculation properties. Chitosan has a pK_a of 6.3–6.5, making it more soluble under acidic conditions because of the protonation of its primary amines. In neutral and alkaline environments, these amines deprotonate, leading to reduced chitosan solubility and a loss of its functional properties. However, by introducing permanent positively charged quaternary ammonium groups, we can overcome the pH-dependent solubility limitations of chitosan, enabling antimicrobial activity across a broad pH range.[5] To confirm the successful quaternization, we determined the zeta potential of the materials in solutions with varying pH levels (3, 6.5, and 8.2). A permanent positive charge indicates successful quaternization (Fig. 2). Compounds containing primary amines (SQC-AETMAC and SQC-GTMAC) displayed changes in their charge with increasing pH. There was a noticeable decrease in charge at pH 6.5 and higher due to the deprotonation of the primary amines at higher pH.[22] In contrast, DQCs exhibited consistently high and permanent positive zeta potential values owing to the abundance of quaternary ammonium groups.

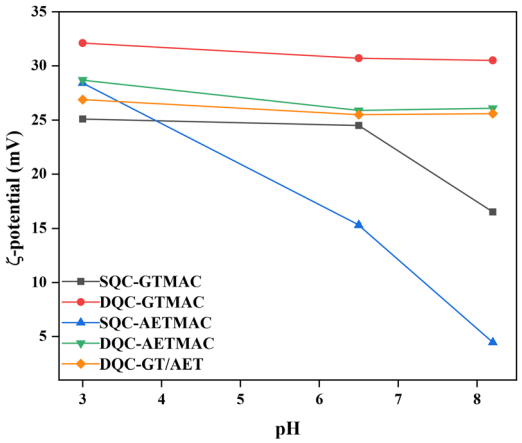

Fig. 2 Zeta potential of various quaternized chitosan derivatives.

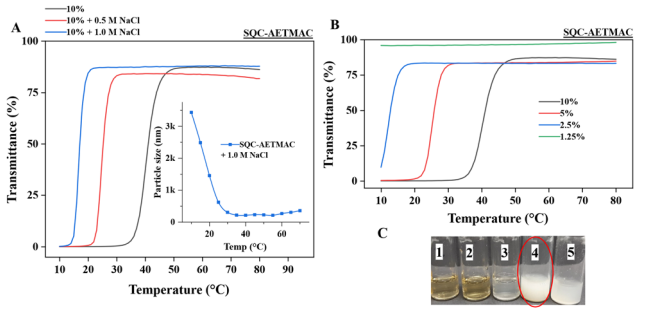

Fig. 3 (A) The influence of NaCl on the UCST behavior of 10% w/v SQC-AETMAC on cooling and consecutively changes in particle size (DLS analysis; inset). (B) The influence of SQC-AETMAC concentration on the UCST behavior on cooling. (C) Photographs of aqueous solutions of different quaternized chitosan derivatives demonstrating differences in solution properties after 10 min, where 1–5 is SQC- and DQC-GTMAC, DQC-GT/AET, SQC- and DQC-AETMAC.

3.1.5. Thermogravimetric analysis (TGA). The thermal degradation was investigated through TGA (Fig. S5A, ESI†). The mass loss of the samples could be divided into two distinct stages. The initial stage, occurring between 30–120 °C, was likely attributed to water evaporation. The second stage, spanning from 120–550 °C, was presumably linked to the degradation of the polysaccharide structure itself due to the cleavage of glycoside linkages and intermolecular bonds.[31] Quaternization resulted in a reduction in the thermostability of chitosan. SQCs exhibited decreased thermostability and residual weight compared to chitosan, while the degradation of DQCs was even more significant. At 800 °C, AETMAC-QCs experienced a greater weight loss compared to GTMAC-QCs. The presence of larger or bulkier functional groups contributed to an additional decrease in thermal stability. A similar trend was observed regarding the number of functional groups present per molecule, with DQC displaying lower stability compared to SQC.

3.1.6. X-ray analysis (XRD). Due to the presence of a considerable number of hydrogen bonds in chitosan and the restriction in the free rotation of the units in each group, chitosan exhibits poor water solubility. This phenomenon can be observed and monitored through XRD to investigate the crystalline structure of chitosan before and after quaternization (Fig. S5B, ESI†). The two characteristic crystalline peaks of chitosan, located at 2θ 12° and 20°, can be considered as crystal reflection angles. The QCs showed a broader peak at approximately 2θ 20–22°, indicating a more amorphous structure. This can be attributed to the introduction of quaternary compounds into the chitosan structure, which interrupts the symmetrical structure of chitosan and the intermolecular and intramolecular hydrogen bonding between –OH and $–NH_2$. As a result, the crystallinity of chitosan is significantly reduced, leading to improved water solubility. These observations are consistent with previous literature.[32,33]

3.1.7. Rheological analysis and solution behavior. Native chitosan dissolves only in an acidic environment, whereas the quaternized chitosan derivatives exhibit good solubility in both neutral and alkaline conditions. Notably, GTMAC-QCs yield a clearer and more homogeneous solution, although they have significantly higher viscosity compared to AETMAC-QCs. The viscosity determines the practical concentrations of the compounds (Fig. S6D, ESI†). Additionally, solution viscosity also affects surface spreading, sprayability, film uniformity, miscibility, and other pertinent factors, where lower viscosities are preferred.

AETMAC-QCs exhibited an upper critical solution temperature-type (UCST) behavior in aqueous solutions at pH 1.2–2.0. This resulted in turbid dispersions at room temperature (25 °C) that became clear upon heating to 80 °C (Fig. 3). In comparison, GTMAC-QCs were readily soluble in water between 10–80 °C and exhibited no thermoresponsive behavior. Both the polymer concentration and the presence of NaCl affected the cloud point (T_{cp}) of SQC-AETMAC. The T_{cp} increased with increasing polymer concentration, from 13 to 41 °C, when the concentration increased from 2.5 to 10% (w/v). No cloud point could be determined for a 1.25% (w/v) solution of SQC-AETMAC (Fig. 3). The presence of NaCl decreased the T_{cp} of a 10% (w/v) solution from 41 °C to 25 and 17 °C, for solutions containing 0.5 and 1.0 M NaCl, respectively (Fig. 3(A)). The clearing points were typically observed at higher temperatures (Fig. S6, ESI†), where also a significant hysteresis in the thermoresponsiveness of SQC-AETMAC was seen. These observations align with what is typically observed for UCST-type polymers in aqueous solutions.[34,35] The T_{cp} of DQC-AETMAC (10% w/v) during the cooling cycle could not be determined. However, a clearing point at 40 °C was observed during the heating cycle (Fig. S6C, ESI†). UCST-type solution behavior was not observed in GTMAC-functionalized QCs or heterogeneously functionalized DQC-GT/AET.

UCST-type solution behavior depends on intra- and intermolecular interactions. These interactions can be hydrogen bonds or electrostatic interactions.[34–36] Due to the low pH of the solutions (1.6–2.0), the primary amines are protonated and the chitosan has a positive charge. Hence, we speculate that the hydrogen bonding of hydroxyls and amines in chitosan with carbonyls in the AETMAC grafts causes aggregation of the polymers, resulting in the UCST-type solution behavior of

SQC-AETMAC. The aggregation can be evaluated with DLS measurements, where large aggregates are observed in the dispersions at temperatures below the T_{cp} (Fig. 3(A) (inset)). By increasing the degree of functionalization and therefore the number of permanent positive charges, the solubility of the chitosan derivatives increased, and the thermoresponsiveness of the material was lost (DQC-AETMAC, DQC-GT/AET). The presence of NaCl increased the solubility of SQC-AETMAC by disrupting the hydrogen bonds, as T_{cp} was shifted to lower temperatures, similar to what has been observed with *e.g.* poly(*N*-acryloylglycinamide).[37] Further studies of the thermoresponsiveness of SQC-AETMAC are needed to fully understand the observed phenomenon.

3.1.8. Antimicrobial activity analysis. All tested QCs demonstrated significant antimicrobial activity against both *P. syringae* and *E. coli-C*. The antimicrobial activity of DQC-AETMAC and SQC-AETMAC derivatives far exceeded that of DQC-GT/AET or DQC-GTMAC against *P. syringae*. All compounds demonstrated a complete inhibition of *P. syringae* up to a concentration of 6.25 mg mL^{-1} (0.6% w/v) of the bioactive molecule (Fig. S7A, ESI†), after a 10 min contact time. DQC-GT/AET demonstrated a decrease in the activity at concentrations lower than 25 mg mL^{-1}. When tested against the more robust organism *E. coli* (Fig. S7B, ESI†), the number of microbial colonies emerging after DQC-AETMAC treatment was significantly lower than after treatment with DQC-GTMAC, indicating higher activity for the former. No colonies were observed with DQC-AETMAC, while several pin-head colonies were present with DQC-GTMAC at a concentration of 100 mg mL^{-1} and after 10 min of contact time. In concentration-dependent activity assay, treatment with 200 mg mL^{-1} of DQC-AETMAC for 10 min demonstrated a 99.99% elimination of viable *E. coli* cells (Fig. S7C, ESI†), although the efficacy was lower at 100 mg mL^{-1}. Similar results were observed in the zone of inhibition assay (Fig. S7D, ESI†), where DQC-AETMAC and DQC-GT/AET derivatives exhibited larger and clearer zones of inhibition compared to DQC-GTMAC derivatives, confirming their positive antimicrobial activity. Sterile distilled water was used as a control agent with no inhibitory effects.

The MIC and MBC (Fig. 4) values were calculated for SQC-AETMAC, DQC-AETMAC, and DQC-GT/AET, which demonstrated the highest activity among all compounds following EUCAST guidelines.[38] The MIC values were determined against Gram-negative *E. coli* and *P. syringae*, as most clinical pathogens are Gram-negative organisms and more challenging to eliminate.[39] SQC-AETMAC showed the highest activity, followed by DQC-AETMAC, with MIC values of 0.78 (0.07% w/v) and 3.12 mg mL^{-1} (0.31% w/v). In contrast, DQC-GT/AET showed a much higher MIC value, at a concentration of 12.5 mg mL^{-1} (1.25% w/v) for >99.5% CFU reduction. Although, at twice the MIC concentration, a complete removal of CFUs was observed (>99.999%), corresponding to MBC as per EUCAST guidelines. The MBC values of SQC-AETMAC were the lowest at 1.5 mg mL^{-1} (0.15% w/v), followed by DQC-AETMAC at 6.25 mg mL^{-1} (0.65% w/v) and DQC-GT/AET at 25.0 mg mL^{-1} (2.5% w/v), demonstrating their high bactericidal

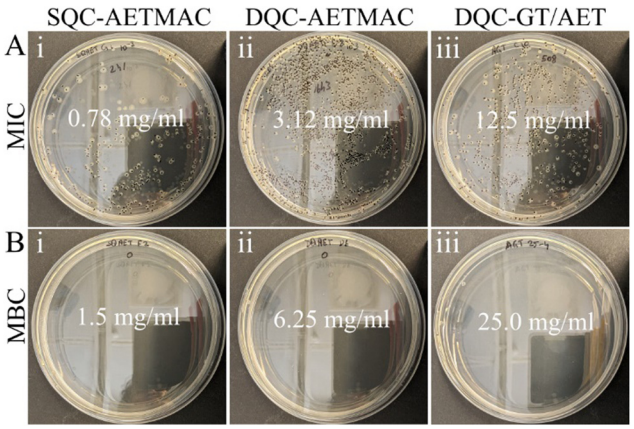

Fig. 4 Antimicrobial activity analysis of quaternized chitosan derivatives on *E. coli*. (A) Photographs showing CFUs observed for (i) SQC-AETMAC; (ii) DQC-AETMAC; and (iii) DQC-GT/AETMAC, and their MIC values (>99.5% inhibition) of 0.78, 3.12, and 12.5 mg mL^{-1} of bioactive molecules after an incubation period of 12 h. (B) Photograph showing antimicrobial activity of (i) SQC-AETMAC; (ii) DQC-AETMAC; and (iii) DQC-GT/AETMAC, and their MBC values of 1.5, 6.25, and 25.0 mg mL^{-1}. No CFUs observed (>99.999% removal; >4 log_{10}) of *E. coli* after 12 h of incubation.

efficacy. According to reports, increasing quaternization and length of alkyl linkers enhance the antibacterial activity against pathogens such as *E. coli*. Furthermore, smaller M_w enhances antibacterial activity against several pathogens.[40] These factors may contribute to the observed high activity in SQC-AETMAC. Further studies are needed to comprehensively evaluate the effect of M_w, linker length, and functional group density on their antibacterial activity.

3.1.9. Cytotoxicity analysis. The cytotoxic tendencies of QCs pose a challenge in their medical applications. Various studies have indicated that toxicity escalates with a higher degree of substitution.[41,42] While the acceptable level of cytotoxicity tolerance can differ based on the specific application, it is essential to strike a balance between optimal antibacterial effect and biocompatibility for certain applications. Here, the cytotoxicity was evaluated on mouse fibroblast cells for various QC concentrations after 24 or 48 h of exposure (Fig. 5 and Fig. S8, ESI†). Notably, at concentrations of 2.0 mg mL^{-1} or higher after a 24 hours exposure, all QCs exhibited noticeable

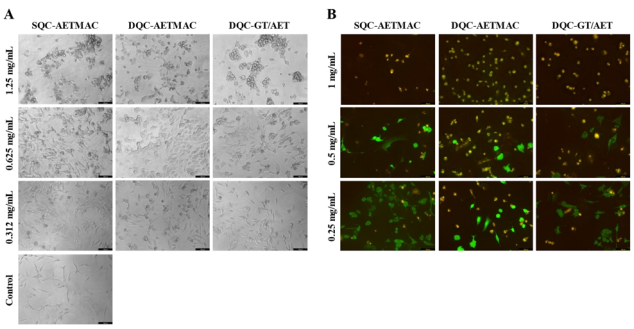

Fig. 5 Cytotoxic behavior of AETMAC-quaternized chitosan on NIH-3T3 fibroblasts at various concentrations after 48 h of incubation; (A) microscopic images, and (B) live/dead analysis (green = alive, red/yellow = dead).

cytotoxicity. This was evident through changes in cell morphology, transitioning from elongated to rounded forms (Fig. 5(A) and Fig. S8B, ESI†), and staining red (PI, dead) during live–dead staining (appearing as yellow, Fig. 5(B)). Changes in cell morphology and viability were also observed at lower concentrations. A decline in viability was more pronounced with a 48 hours exposure, indicating a concentration and time-dependent cytotoxic influence. Most compounds demonstrated an LD_{50} value around 0.50 mg mL^{-1}; below this threshold, the cytotoxicity remained relatively low, characterized by extended cell morphology and a larger number of cells staining green (FDA) in live–dead analysis. In MTT-based viability assessment, cells exhibited approximately 50% viability (Fig. S8A, ESI†), compared to the control at 0.5 mg mL^{-1}, even after 48 h of exposure. DQC-GT/AET displayed higher cell viability after both 24 and 48 h compared to SQC- and DQC-AETMAC, indicating its marginally lower cytotoxicity relative to the other two compounds. This difference could be attributed to the presence of heterogeneous functional groups and structural differences. DQC-GT/AET exhibited approximately 60% cell viability at 0.5 mg mL^{-1} and over 75% cell viability at 0.25 mg mL^{-1} after 48 h of exposure. In contrast, the cell viability was comparatively lower for the other two compounds (Table S1, ESI†).

Considering the antibacterial analysis, the concentrations required for complete bacterial removal fell within the range of cytotoxicity for both DQC-AETMAC and DQC-GT/AET. In the case of SQC-AETMAC, the MIC concentrations were slightly below the threshold of inducing excessive cell death. Nevertheless, in applications where direct chitosan-tissue contact is not essential – such as in surface disinfectants and specific wound coverings or healing films – cytotoxicity becomes a minor concern. Here, these QCs can be sustainable and viable alternatives with long-lasting inherent antibacterial activity, *e.g.* for environmental and plant pathogen control applications. Research on these properties of QC and applications demanding higher specificity is necessary for developing environmentally safe and sustainable antimicrobial agents.

4. Conclusion

This study presents a method for synthesizing quaternary chitosan compounds, offering an antibacterial alternative to previously quaternized chitosan derivatives and other antimicrobial agents. The incorporation of the quaternary compound AETMAC into chitosan resulted in structures featuring a permanent positive charge over a wide pH range. Comparative analysis between AETMAC-QCs and GTMAC-QCs revealed distinctive structure–property relationships. Notably, GTMAC derivatives exhibited significantly higher viscosity and molecular weight, limiting higher-concentration handling. Conversely, AETMAC-functionalized compounds exhibited substantially reduced viscosity, mitigating limitations associated with concentration-dependent applications and solubility, thus enhancing practicality. Notably, single quaternized SQC-AETMAC exhibited an Upper Critical Solution Temperature (UCST) behavior, a novel finding in cationically functionalized chitosan, as far as our knowledge goes. Antimicrobial assessment against model organisms *P. syringae* and *E. coli* revealed positive results, with AETMAC-functionalized materials demonstrating superior activity (99.99% removal) compared to GTMAC derivatives. Particularly, SQC-AETMAC exhibited the lowest MIC and MBC values, with >4 $\log_{10}$ removal of *E. coli*, demonstrating its potent antibacterial potential for surface disinfection. The antibacterial properties of quaternary chitosan are attributed to factors such as positive charge, low molecular weight, linker length, and functional group characteristics, warranting further exploration in future studies. While mammalian cell cytotoxicity assays revealed increased cytotoxicity with higher chitosan concentrations and prolonged exposure, it's important to note that the relevance of such cytotoxicity should be considered context-specific rather than generalized across all applications. This approach of synthesizing quaternary chitosan provides an alternative to existing methods, generating quaternary compounds with excellent antibacterial activity suitable for various applications, including surface disinfection, antimicrobial surfaces, and biomedical or environmental use.

Author contributions

Conceptualization: S. B., A. T., and J. S.; methodology: S. B., I. L., A. T., and J. N.; investigation: S. B., I. L., and A. T.; writing (original draft): S. B., I. L., A. T., J. N.; writing (review and editing): I. L., A. T., J. N., and J. S.; supervision: J. S.; funding and acquisition: J. S.

Conflicts of interest

There are no conflicts to declare.

Acknowledgements

The authors would like to thank the Academy of Finland (project number 1333-55163 SA/COVID-19) for providing funding for this project. I. L. would like to thank Svenska Kulturfonden for a PhD scholarship (grant number 167114). This work made use of the BIOECONOMY infrastructure at Aalto University.

References

1 M. Kołodziejska, K. Jankowska, M. Klak and M. Wszoła, Chitosan as an Underrated Polymer in Modern Tissue Engineering, *Nanomater.*, 2021, **11**(11), 3019, DOI: **10.3390/nano11113019**.
2 V. Zargar, M. Asghari and A. Dashti, A Review on Chitin and Chitosan Polymers: Structure, Chemistry, Solubility, Derivatives, and Applications, *ChemBioEng Rev.*, 2015, **2**(3), 204–226.

3 Y. Qin and P. Li, Antimicrobial Chitosan Conjugates: Current Synthetic Strategies and Potential Applications, *Int. J. Mol. Sci.*, 2020, **21**(2), 499, DOI: **10.3390/ijms21020499**.
4 M. A. Sajid, S. A. Shahzad, F. Hussain, W. G. Skene, Z. A. Khan and M. Yar, Synthetic Modifications of Chitin and Chitosan as Multipurpose, *Biopolymers: A Review. Synth. Commun.*, 2018, **48**(15), 1893–1908.
5 P. Sahariah and M. Másson, Antimicrobial Chitosan and Chitosan Derivatives: A Review of the Structure-Activity Relationship, *Biomacromolecules*, 2017, **18**(11), 3846–3868, DOI: **10.1021/acs.biomac.7b01058**.
6 B. I. Andreica, X. Cheng and L. Marin, Quaternary Ammonium Salts of Chitosan. A Critical Overview on the Synthesis and Properties Generated by Quaternization, *Eur. Polym. J.*, 2020, **139**, 110016, DOI: **10.1016/j.eurpolymj.2020.110016**.
7 T. Xu, M. Xin, M. Li, H. Huang, S. Zhou and J. Liu, Synthesis, Characterization, and Antibacterial Activity of N,O-Quaternary Ammonium Chitosan, *Carbohydr. Res.*, 2011, **346**(15), 2445–2450, DOI: **10.1016/j.carres.2011.08.002**.
8 M. Másson, Antimicrobial Properties of Chitosan and Its Derivatives, *Adv. Polym. Sci.*, 2021, 131–168, DOI: **10.1007/12_2021_104**.
9 Z. Cele, L. Ndlandla, A. Somboro, D. Gyamfi and M. Balogun, Synthesis, Characterization and Antimicrobial Activities of Quaternary Chitosan-Based Materials, *IOP Conference Series: Materials Science and Engineering*, IOP Publishing, 2018, vol. 430, p. 12048.
10 W. Y. Cheah, P.-L. Show, I.-S. Ng, G.-Y. Lin, C.-Y. Chiu and Y.-K. Chang, Antibacterial Activity of Quaternized Chitosan Modified Nanofiber Membrane, *Int. J. Biol. Macromol.*, 2019, **126**, 569–577.
11 E. D. Freitas, C. F. Moura Jr, J. Kerwald and M. M. Beppu, An Overview of Current Knowledge on the Properties, Synthesis and Applications of Quaternary Chitosan Derivatives, *Polymers*, 2020, **12**(12), 2878.
12 C. Qin, Q. Xiao, H. Li, M. Fang, Y. Liu, X. Chen and Q. Li, Calorimetric Studies of the Action of Chitosan-*N*-2-Hydroxypropyl Trimethyl Ammonium Chloride on the Growth of Microorganisms, *Int. J. Biol. Macromol.*, 2004, **34**(1–2), 121–126, DOI: **10.1016/j.ijbiomac.2004.03.009**.
13 M. M. Hassan, Enhanced Antimicrobial Activity and Reduced Water Absorption of Chitosan Films Graft Copolymerized with Poly(Acryloyloxy)Ethyltrimethylammonium Chloride, *Int. J. Biol. Macromol.*, 2018, **118**, 1685–1695, DOI: **10.1016/j.ijbiomac.2018.07.013**.
14 H. Sashiwa, N. Yamamori, Y. Ichinose, J. Sunamoto and S. I. Aiba, Michael Reaction of Chitosan with Various Acryl Reagents in Water, *Biomacromolecules*, 2003, **4**(5), 1250–1254, DOI: **10.1021/bm030022o**.
15 J. D. Katiyar and S. Chattopadhyay, Quantitative Functionalization of Chitosan Using Green and Efficient Azetidinium-Amine Reactions, *Carbohydr. Polym.*, 2022, **287**, 119324, DOI: **10.1016/j.carbpol.2022.119324**.
16 A. Teotia, I. Lauren, S. Borandeh and J. Seppala, Quaternized Chitosan Derivatives as Viable Antiviral Agents: 2 Structure – Activity Correlations and Mechanisms of Action, *ACS Appl. Mater. Interfaces*, 2023, **15**, 18707–18719, DOI: **10.1021/acsami.3c01421**.
17 X. Fu, Y. Shen, X. Jiang, D. Huang and Y. Yan, Chitosan Derivatives with Dual-Antibacterial Functional Groups for Antimicrobial Finishing of Cotton Fabrics, *Carbohydr. Polym.*, 2011, **85**(1), 221–227, DOI: **10.1016/j.carbpol.2011.02.019**.
18 V. A. Spinelli, M. C. M. Laranjeira and V. T. Fávere, Preparation and Characterization of Quaternary Chitosan Salt: Adsorption Equilibrium of Chromium(VI) Ion, *React. Funct. Polym.*, 2004, **61**(3), 347–352, DOI: **10.1016/j.reactfunctpolym.2004.06.010**.
19 J. Schindelin, I. Arganda-Carreras, E. Frise, V. Kaynig, M. Longair, T. Pietzsch, S. Preibisch, C. Rueden, S. Saalfeld, B. Schmid, J.-Y. Tinevez, D. J. White, V. Hartenstein, K. Eliceiri, P. Tomancak and A. Cardona, Fiji: An Open-Source Platform for Biological-Image Analysis, *Nat. Methods*, 2012, **9**(7), 676–682, DOI: **10.1038/nmeth.2019**.
20 H. Li, Y. Du, X. Wu and H. Zhan, Effect of Molecular Weight and Degree of Substitution of Quaternary Chitosan on Its Adsorption and Flocculation Properties for Potential Retention-Aids in Alkaline Papermaking, *Colloids Surf., A*, 2004, **242**(1–3), 1–8, DOI: **10.1016/j.colsurfa.2004.04.051**.
21 D. Martins dos Santos, A. de Lacerda Bukzem and S. P. Campana-Filho, *Response Surface Methodology Applied to the Study of the Microwave-Assisted Synthesis of Quaternized Chitosan*, Elsevie Ltd., Sao Carlos, Brazil, 2016, pp. 317–326, DOI: **10.1016/j.carbpol.2015.11.056**.
22 K. Y. Chen and S. Y. Zeng, Fabrication of Quaternized Chitosan Nanoparticles Using Tripolyphosphate/Genipin Dual Cross-Linkers as a Protein Delivery System, *Polymers*, 2018, **10**(11), 1226, DOI: **10.3390/polym10111226**.
23 A. Hirai, H. Odani and A. Nakajima, Determination of Degree of Deacetylation of Chitosan by ^{1}H NMR Spectroscopy, *Polym. Bull.*, 1991, **26**(1), 87–94, DOI: **10.1007/BF00299352**.
24 Y. D. Soubaneh, S. Ouellet, C. Dion and J. Gagnon, Formation of Highly Quaternized *N*,*N*,*N*-Trimethylchitosan: A Chemoselective Methodology in Aqueous Media, *Pure Appl. Chem.*, 2019, **91**(3), 489–496, DOI: **10.1515/pac-2018-0924**.
25 I. Aranaz, A. R. Alcántara, M. C. Civera, C. Arias, B. Elorza, A. H. Caballero and N. Acosta, Chitosan: An Overview of Its Properties and Applications, *Polymers*, 2021, **13**(19), 3256, DOI: **10.3390/polym13193256**.
26 R. J. Nordtveit Hjerde, K. M. Vårum, H. Grasdalen, S. Tokura and O. Smidsrød, Chemical Composition of O-(Carboxymethyl)-Chitins in Relation to Lysozyme Degradation Rates, *Carbohydr. Polym.*, 1997, **34**(3), 131–139, DOI: **10.1016/s0144-8617(97)00113-6**.
27 V. N. Davydova, V. P. Nagorskaya, V. I. Gorbach, A. A. Kalitnik, A. V. Reunov, T. F. Solov'eva and I. M. Ermak, Chitosan Antiviral Activity: Dependence on Structure and Depolymerization Method, *Appl. Biochem. Microbiol.*, 2011, **47**(1), 103–108, DOI: **10.1134/S0003683811010042**.
28 M. Iriti and E. M. Varoni, Chitosan-Induced Antiviral Activity and Innate Immunity in Plants, *Environ. Sci. Pollut. Res.*, 2015, **22**(4), 2935–2944, DOI: **10.1007/s11356-014-3571-7**.
29 S. N. Kulikov, S. N. Chirkov, A. V. Il'ina, S. A. Lopatin and V. P. Varlamov, Effect of the Molecular Weight of Chitosan

on Its Antiviral Activity in Plants, *Appl. Biochem. Microbiol.*, 2006, **42**(2), 200–203, DOI: **10.1134/S0003683806020165**.

30 N. R. Sudarshan, D. G. Hoover and D. Knorr, Antibacterial Action of Chitosan, *Food Biotechnol.*, 1992, **6**(3), 257–272.

31 A. Sarwar, H. Katas, S. N. Samsudin and N. M. Zin, Regioselective Sequential Modification of Chitosan via Azide-Alkyne Click Reaction: Synthesis, Characterization, and Antimicrobial Activity of Chitosan Derivatives and Nanoparticles, *PLoS One*, 2015, **10**(4), DOI: **10.1371/journal.pone.0123084**.

32 L. Sun, Y. Du, L. Fan, X. Chen and J. Yang, Preparation, Characterization and Antimicrobial Activity of Quaternized Carboxymethyl Chitosan and Application as Pulp-Cap, *Polymer*, 2006, **47**(6), 1796–1804, DOI: **10.1016/j.polymer.2006.01.073**.

33 J. Luo, X. Wang, B. Xia and J. Wu, Preparation and Characterization of Quaternized Chitosan under Microwave Irradiation, *J. Macromol. Sci., Part A: Pure Appl. Chem.*, 2010, **47**(9), 952–956, DOI: **10.1080/10601325.2010.501310**.

34 J. Niskanen, J. Vapaavuori, C. Pellerin, F. M. Winnik and H. Tenhu, Polysulfobetaine-Surfactant Solutions and Their Use in Stabilizing Hydrophobic Compounds in Saline Solution, *Polymer*, 2017, **127**, 77–87, DOI: **10.1016/j.polymer.2017.08.057**.

35 J. Seuring, F. M. Bayer, K. Huber and S. Agarwal, Upper Critical Solution Temperature of Poly(*N*-Acryloyl Glycinamide) in Water: A Concealed Property, *Macromolecules*, 2012, **45**(1), 374–384, DOI: **10.1021/ma202059t**.

36 P. Mary, D. D. Bendejacq, M. P. Labeau and P. Dupuis, Reconciling Low- and High-Salt Solution Behavior of Sulfobetaine Polyzwitterions, *J. Phys. Chem. B*, 2007, **111**(27), 7767–7777, DOI: **10.1021/jp071995b**.

37 F. Liu, J. Seuring and S. Agarwal, Atom Transfer Radical Polymerization as a Tool for Making Poly(*N*-Acryloylglycinamide) with Molar Mass Independent UCST-Type Transitions in Water and Electrolytes, *Polym. Chem.*, 2013, **4**(10), 3123–3131, DOI: **10.1039/c3py00222e**.

38 EUCAST. **https://www.eucast.org/**.

39 B. Jubeh, Z. Breijyeh and R. Karaman, Resistance of Gram-positive Bacteria to Current Antibacterial Agents and Overcoming Approaches, *Molecules*, 2020, **25**(12), 2888, DOI: **10.3390/molecules25122888**.

40 P. Sahariah, B. E. Benediktssdóttir, M. A. Hjálmarsdóttir, O. E. Sigurjonsson, K. K. Sørensen, M. B. Thygesen, K. J. Jensen and M. Másson, Impact of Chain Length on Antibacterial Activity and Hemocompatibility of Quaternary *N*-Alkyl and *N*,*N*-Dialkyl Chitosan Derivatives, *Biomacromolecules*, 2015, **16**(5), 1449–1460, DOI: **10.1021/acs.biomac.5b00163**.

41 A. Zubareva, B. Shagdarova, V. Varlamov, E. Kashirina and E. Svirshchevskaya, Penetration and Toxicity of Chitosan and Its Derivatives, *Eur. Polym. J.*, 2017, **93**, 743–749, DOI: **10.1016/j.eurpolymj.2017.04.021**.

42 E. Faizuloev, A. Marova, A. Nikonova, I. Volkova, M. Gorshkova and V. Izumrudov, Water-Soluble N-[(2-Hydroxy-3-Trimethylammonium)Propyl]Chitosan Chloride as a Nucleic Acids Vector for Cell Transfection, *Carbohydr. Polym.*, 2012, **89**(4), 1088–1094, DOI: **10.1016/j.carbpol.2012.03.071**.